Materials Transactions, Vol. 51, No. 3 (2010) pp. 535 to 541

Detection of Neodymium-Rich Phase for Development of Coercivity in Neodymium-Iron-Boron-Based Alloys with Submicron-Sized Grains Using Positron Lifetime Spectroscopy

Takeshi Nishiuchi[1,2,*], Masaki Nakamura[2,*], Satoshi Hirosawa[1], Masataka Mizuno[2], Hideki Araki[2] and Yasuharu Shirai[3]

[1]*Magnetic Materials Research Laboratory, NEOMAX Company, Hitachi Metals, Ltd., Mishima-gun, Osaka 618-0013, Japan*
[2]*Graduate School of Engineering, Osaka University, Suita 565-0871, Japan*
[3]*Graduate School of Engineering, Kyoto University, Kyoto 606-8501, Japan*

In order to evaluate the relationship between positron lifetime and microstructure, which contributes to the development of coercivity in hydrogenation-disproportionation-desorption-recombination (HDDR)-processed Nd-Fe-B-based alloys, detailed studies of positron lifetime spectroscopy were performed on HDDR-processed Nd-Fe-B-based alloys during desorption-recombination (DR) treatment. After the onset of coercivity, the change in positron lifetime closely corresponded to the change in intrinsic coercivity (H_{cJ}) with the progress of DR treatment. This result can be explained in terms of the grain size of the recombined $Nd_2Fe_{14}B$ phases and the diffusion length of positrons, which annihilate in the matrix before reaching the grain boundary. Furthermore, positron lifetime spectroscopy was able to detect small changes in the grain boundary region very sensitively compared with thermal desorption spectroscopy (TDS) and X-ray diffraction (XRD). These changes in the grain boundary region caused the onset of coercivity attributed to the formation of Nd-rich intergranular phases. These results indicate that formation of a small amount of the Nd-rich intergranular phase during the DR process, which could be detected by positron lifetime spectroscopy, contributes to the onset of coercivity, even if NdH_x phases remain. [doi:10.2320/matertrans.M2009342]

(Received October 13, 2009; Accepted December 28, 2009; Published February 17, 2010)

Keywords: *positron lifetime spectroscopy, neodymium-iron-boron-based alloy, hydrogenation-disproportionation-desorption-recombination process, coercivity, neodymium-rich phase*

1. Introduction

Positron lifetime spectroscopy[1–3] is a unique technique for obtaining information on the structural characteristics of positron annihilation sites, typically atomic-scale lattice defects such as vacancies, dislocations and grain boundaries, from a large region of a sample. Therefore, characterization of materials by positron lifetime spectroscopy is often useful for obtaining a deeper understanding of microstructural evolution in metal processing. Using this technique, we have recently investigated the microstructural evolution in hydrogenation-disproportionation-desorption-recombination (HDDR) processing[4,5] for the fabrication of Nd-Fe-B magnets with submicron-sized grains (typical grain size is 200 to 500 nm). In our previous studies,[6–8] the positron lifetime in samples processed by desorption-recombination (DR) treatment for various times from 0 to 30 min were measured in order to discuss the relationship between microstructural changes and the development of coercivity in HDDR-processed Nd-Fe-B-based alloys. The results revealed that at least some positrons annihilate in the Nd-rich intergranular phase newly formed in the sample after the coercivity was sharply increased by DR treatment.

In this paper, in order to demonstrate the usefulness of positron lifetime spectroscopy for the detection of the Nd-rich phase in HDDR-processed Nd-Fe-B alloy, we investigated the relationship between coercivity and positron lifetime for a wider range of DR treatment times compared with our previous works,[6–8] and conducted a detailed comparison between positron lifetime spectroscopy and other methods such as X-ray diffraction (XRD) and magneto-optical Kerr effect (MOKE) microscopy, especially around the DR treatment time at which coercivity sharply increased. Furthermore, we evaluated the contribution of the formation of the Nd-rich phase to coercivity development during DR treatment.

2. Experimental Procedure

$Nd_{12.5}Fe_{73-x}Co_8B_{6.5}Ga_x$ homogenized ingots with Ga composition (x) of 0 and 0.2 (mol%) were annealed at 1110°C for 16 h in an argon atmosphere and mechanically pulverized to obtain starting alloy powders. HDDR treatment was applied to the starting powders as described below. First, the powders were heated to 840°C under an argon gas flow at atmospheric pressure. The powders were then exposed to a hydrogen gas flow at atmospheric pressure and 840°C for 4 h to conduct the HD treatment. Subsequently, the powders were exposed to an argon gas flow at 5.33 kPa and 840°C for the DR treatment. Only the DR treating times (t_{DR}) of the samples were varied, ranging from 0 to 480 min. The intrinsic coercivity of the HDDR-processed alloy samples was measured with a vibrating sample magnetometer (VSM) without demagnetization correction. Positron lifetime spectroscopy was performed using a fast-fast timing coincidence system with a time resolution (FWHM) of 190 ps. A 50 μCi positron source of ^{22}Na was put into the sample powder. The positron source contribution and the resolution function were evaluated by using the code RESOLUTION.[9] The positron lifetime spectra were analyzed using the POSITRONFIT EXTENDED program.[10,11] Thermal desorption spectroscopy (TDS) was used to estimate the hydrogen

*Graduate Student, Osaka University

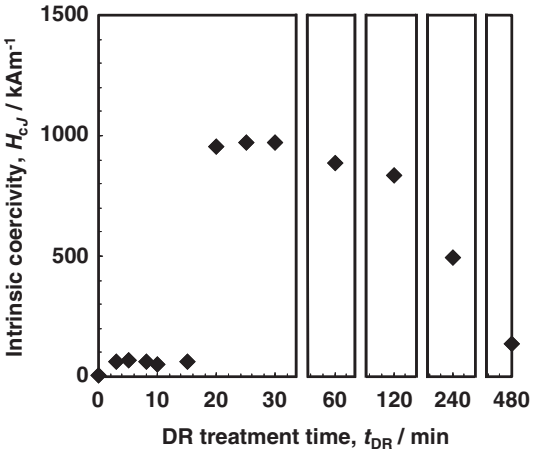

Fig. 1 Relationship between intrinsic coercivity (H_{cJ}) of samples and DR treatment time (t_{DR}) for $Nd_{12.5}Fe_{73}Co_8B_{6.5}$ alloy after HD treatment at 840°C for 4 h.

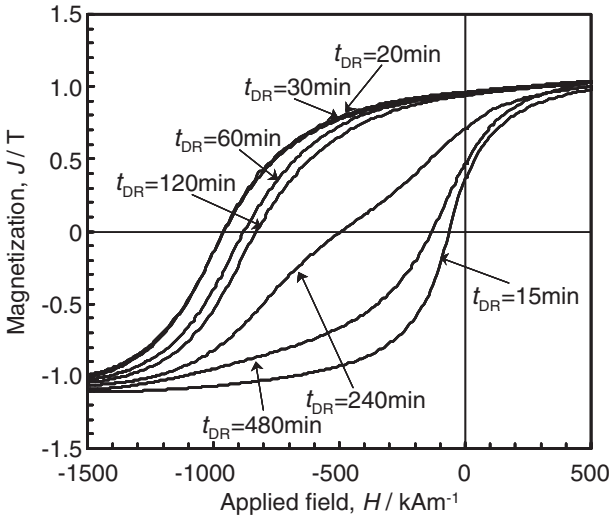

Fig. 2 Demagnetization curves of $Nd_{12.5}Fe_{73}Co_8B_{6.5}$ alloy at DR treatment times (t_{DR}) of 15 to 480 min after HD treatment at 840°C for 4 h.

content in the samples and X-ray diffraction (XRD) analysis was carried out to identify constituent phases. Cross sections of the samples were observed by magneto-optical Kerr effect (MOKE) microscopy to conduct a microstructural investigation.

3. Results

3.1 Coercivity and positron lifetime changes during DR treatment for t_{DR} = 0 to 480 min

3.1.1 Magnetic properties of samples

Figure 1 shows the intrinsic coercivity (H_{cJ}) of the HDDR-processed $Nd_{12.5}Fe_{73}Co_8B_{6.5}$ alloy with no Ga addition as a function of DR time, and Fig. 2 shows demagnetization curves of the samples at various DR treatment times (t_{DR}) from 15 to 480 min. In our previous studies,[6–8] we have shown that in a narrow DR time range of 0 to 30 min, the DR process can be divided into three stages with respect to the change in H_{cJ}: (1) t_{DR} = 0 to 15 min (Stage I), (2) t_{DR} = 15 to 20 min (Stage II) and (3) t_{DR} = 20 to 30 min (Stage III). As shown in Fig. 1, H_{cJ} remains low during Stage I and abruptly increases from 63 kA/m to 957 kA/m during Stage II. During Stage III, H_{cJ} maintains an elevated level, and the shape of demagnetization curve remains almost unchanged, as shown in Fig. 2. Previous studies reported by the authors[6–8] and Li *et al.*[12,13] have shown that Nd-rich intergranular phases form between recombined $Nd_2Fe_{14}B$ phases and these Nd-rich phases cause the development of coercivity in Stage II.

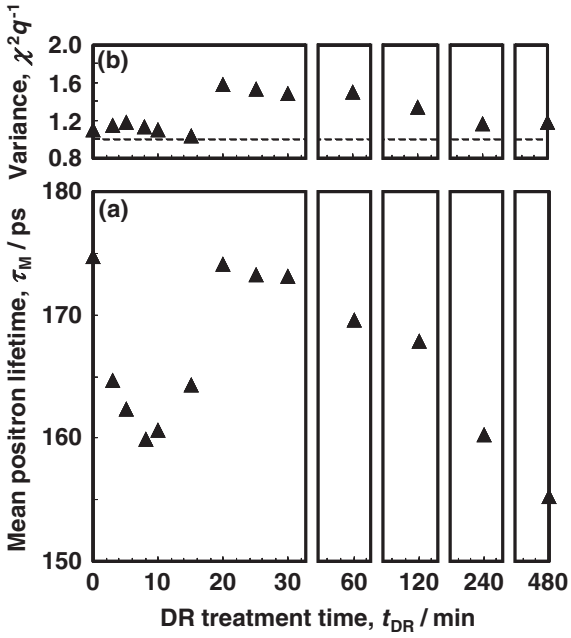

Fig. 3 Results of positron lifetime spectroscopy of samples at various DR treatment time (t_{DR}) for $Nd_{12.5}Fe_{73}Co_8B_{6.5}$ alloy after HD treatment at 840°C for 4 h: (a) mean positron lifetime (τ_M), (b) variance (χ^2q^{-1}).

In the present study, we expanded the DR time range as shown in Figs. 1 and 2. In the period of t_{DR} = 30 to 120 min, H_{cJ} gradually decreased while the remanence (J_r) remained almost unchanged. We also found that at t_{DR} = 240 min, the squareness of the demagnetization curve in the second quadrant was lost and a large decrease in H_{cJ} occurred. At t_{DR} = 480 min, the magnetic moment in the sample was easily reversed in a low magnetic field such that both J_r and H_{cJ} became extremely low. Thus, we refer to the period of t_{DR} = 30 to 480 min as Stage IV hereinafter.

3.1.2 Positron lifetime of samples

Figure 3(a) shows the mean positron lifetime (τ_M) which was estimated by fitting the measured spectrum with $T(t)$ as a function of positron annihilation time t, using eq. (1),

$$T(t) = \frac{1}{\tau_M}\exp\left(-\frac{t}{\tau_M}\right). \quad (1)$$

Here, we consider the time resolution of the measurement system and the contribution of positron annihilation in the positron source. Figure 3(b) also shows the "variance" (χ^2q^{-1}) of the spectral fitting calculated using eq. (1).

In this study, if χ^2q^{-1} was in the range from 0.9 to 1.1, it was assumed that fitting of the spectrum was successful and all of the positron annihilation sites had the same characteristics. On the other hand, if χ^2q^{-1} was greater than 1.2, it was assumed that the measured spectrum should be fitted in two or more components of positron lifetime.

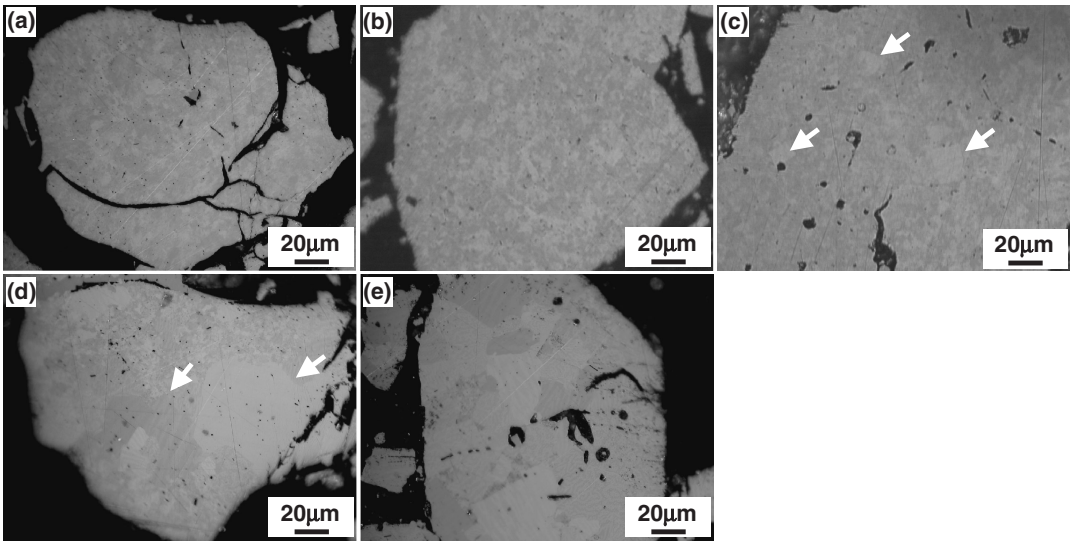

Fig. 4 Cross-sectional MOKE images of samples at various DR treatment time (t_{DR}) for $Nd_{12.5}Fe_{73}Co_8B_{6.5}$ alloy after HD treatment at 840°C for 4 h: (a) $t_{DR} = 30$ min, (b) $t_{DR} = 60$ min, (c) $t_{DR} = 120$ min, (d) $t_{DR} = 240$ min and (e) $t_{DR} = 480$ min. White arrows indicate large grains caused by undesired grain growth.

In Stage I, τ_M rapidly decreased and then increased. On the contrary, $\chi^2 q^{-1}$ was almost 1.0 for all t_{DR} in this stage. Then, $\chi^2 q^{-1}$ abruptly increased to 1.6 and τ_M increased to 174 ps at $t_{DR} = 20$ min in Stage II. These values maintained a high level in Stage III, as reported in previous studies.[6–8] These results were interpreted to indicate that new positron annihilation sites with τ_M of more than 174 ps formed at $t_{DR} = 20$ min, and that there were two or more types of positron annihilation sites in the sample. The new positron annihilation sites were related to the formation of Nd-rich intergranular phases,[7,12] which caused the sudden onset of coercivity in Stage II, as described above.

In contrast, during Stage IV, τ_M and $\chi^2 q^{-1}$ gradually decreased from 173 to 155 ps and from 1.6 to less than 1.2, respectively, as H_{cJ} gradually decreased from 973 to 134 kA/m. Over a wide DR time range from 15 min (Stage II) to 480 min (Stage IV) the changes in τ_M and $\chi^2 q^{-1}$ were similar to that in H_{cJ}. The typical diffusion length of a positron in the matrix was on the order of 10^{-7} m, which was similar to the grain size of a typical HDDR-processed alloy. Thus, some of the positrons were expected to annihilate in the matrix of the $Nd_2Fe_{14}B$ phase. In order to estimate the positron lifetime in the matrix of the $Nd_2Fe_{14}B$ phase, we also measured the positron lifetime of the starting alloy with the same composition, which consisted of large $Nd_2Fe_{14}B$ grains of around 100 μm or more. The results showed that $\tau_M = 157$ ps. These grain sizes were much larger than the diffusion length of positrons from injection to annihilation in the matrix; thus, almost all of the positrons were expected to annihilate in the matrix.

3.1.3 Microstructural changes in samples after $t_{DR} = 30$ min

In order to understand why the changes of coercivity and positron lifetime showed good agreement in Stage IV, MOKE microscopy was used to observe cross sections of each sample for various t_{DR}; the results are shown in Fig. 4. The complex patterns of contrast were caused by the magnetic domain structures. The MOKE image of the sample with $t_{DR} = 30$ min (Fig. 4(a)) shows very fine magnetic domains, similar to those observed in typical HDDR-processed Nd-Fe-B magnets with submicron-sized grains.[14] On the other hand, the volume fraction of large grains with sizes of 10 μm or more gradually increased, and stripe-like contrast of magnetic domains, similar to those typically observed in a Nd-Fe-B cast ingot, became dominant as DR treatment progressed (Figs. 4(b)–(d)).

3.2 Comparison of changes in positron lifetime, microstructure and coercivity between $Nd_{12.5}Fe_{73}Co_8B_{6.5}$ and $Nd_{12.5}Fe_{72.8}Co_8B_{6.5}Ga_{0.2}$

3.2.1 Magnetic properties

In order to study the relationship between positron lifetime and coercivity in Stage II closely, we prepared a new alloy with a small amount of Ga addition ($Nd_{12.5}Fe_{72.8}Co_8B_{6.5}Ga_{0.2}$), which we processed for various DR treatment times. In this experiment, the t_{DR} was changed from 0 to 30 min in 2-min increments over the range of $t_{DR} = 8$ to 24 min, which included times before and after the onset of coercivity.

Figure 5 shows intrinsic coercivity (H_{cJ}) of the HDDR-processed $Nd_{12.5}Fe_{73}Co_8B_{6.5}$ (no Ga addition) and $Nd_{12.5}Fe_{72.8}Co_8B_{6.5}Ga_{0.2}$ (Ga addition) alloys as a function of DR treatment time, and Figs. 6(a) and (b) also show changes in the demagnetization curves in the range of $t_{DR} = 12$ to 18 min for $Nd_{12.5}Fe_{73}Co_8B_{6.5}$ and $Nd_{12.5}Fe_{72.8}Co_8B_{6.5}Ga_{0.2}$. Similar to the $Nd_{12.5}Fe_{73}Co_8B_{6.5}$ alloy, H_{cJ} of the $Nd_{12.5}Fe_{72.8}Co_8B_{6.5}Ga_{0.2}$ alloy sharply increased from 48 to 1332 kA/m in the specific period of DR treatment (*i.e.*, $t_{DR} =$ 12 to 18 min). The alloy with a small amount of Ga reached a higher H_{cJ} than that without Ga, showing good agreement with previous reports.[5,15]

A careful comparison of H_{cJ} and the demagnetization curves for $Nd_{12.5}Fe_{73}Co_8B_{6.5}$ and $Nd_{12.5}Fe_{72.8}Co_8B_{6.5}Ga_{0.2}$ alloys showed that at $t_{DR} = 14$ min, the demagnetization curve of $Nd_{12.5}Fe_{73}Co_8B_{6.5}$ alloy was the same as that of $t_{DR} = 12$ min and H_{cJ} maintained a low level (51 kA/m) that

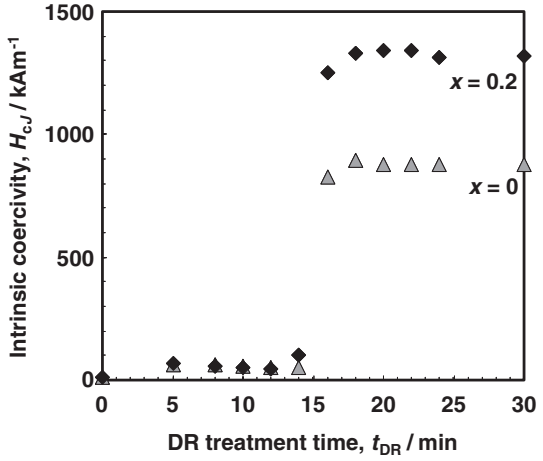

Fig. 5 Relationship between intrinsic coercivity (H_{cJ}) and DR treatment time (t_{DR}) for $Nd_{12.5}Fe_{73-x}Co_8B_{6.5}Ga_x$ ($x = 0, 0.2$) alloys after HD treatment at 840°C for 4 h.

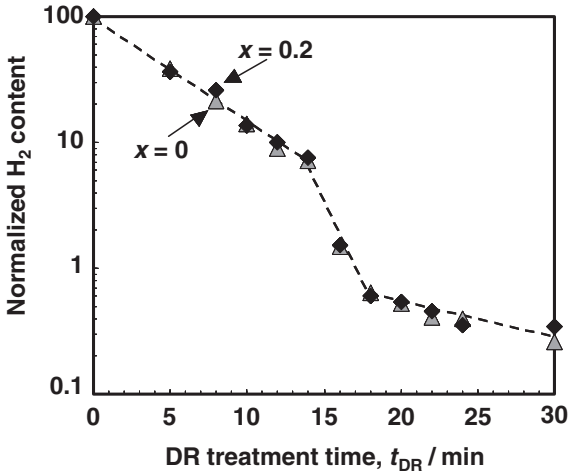

Fig. 7 Relationship between normalized hydrogen content of samples and DR treatment time (t_{DR}) for $Nd_{12.5}Fe_{73-x}Co_8B_{6.5}Ga_x$ ($x = 0, 0.2$) alloys after HD treatment at 840°C for 4 h. For each alloy, hydrogen content at $t_{DR} = 0$ min is set at 100.

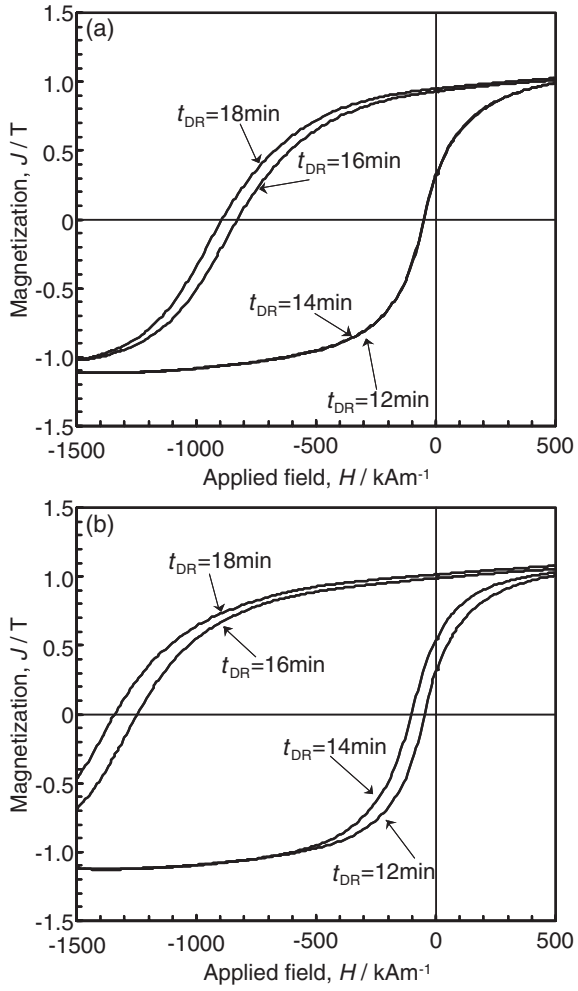

Fig. 6 Demagnetization curves of samples of (a) $Nd_{12.5}Fe_{73}Co_8B_{6.5}$ and (b) $Nd_{12.5}Fe_{72.8}Co_8B_{6.5}Ga_{0.2}$ alloys at DR treatment times (t_{DR}) of 12 to 18 min after HD treatment at 840°C for 4 h.

was equal to that at $t_{DR} = 12$ min or less. On the other hand, the demagnetization curve of $Nd_{12.5}Fe_{72.8}Co_8B_{6.5}Ga_{0.2}$ considerably changed and H_{cJ} slightly increased from 48 to 102 kA/m in the period from $t_{DR} = 12$ to 14 min. These results indicate that Ga addition to a Nd-Fe-B-based alloy accelerated the onset of coercivity caused by the HDDR process.

3.2.2 Residual hydrogen concentrations

The residual hydrogen concentrations, C, in the samples that were measured by TDS for the $Nd_{12.5}Fe_{73}Co_8B_{6.5}$ and $Nd_{12.5}Fe_{72.8}Co_8B_{6.5}Ga_{0.2}$ alloys are shown in Fig. 7. In this figure, C is normalized with the value at $t_{DR} = 0$ min and plotted on a logarithmic scale. As shown in Fig. 7, the hydrogen desorption during DR treatment appears to be described by three first-order reactions with different coefficients of k_i ($i = 1, 2, 3$) in the following equation,

$$\frac{\partial C}{\partial t} = -k_i C. \tag{2}$$

There was little difference in the time variation of C between the $Nd_{12.5}Fe_{73}Co_8B_{6.5}$ and $Nd_{12.5}Fe_{72.8}Co_8B_{6.5}Ga_{0.2}$ alloys. Both of the alloys had almost the same three kinetic coefficients, namely, $k_1 \approx 0.08\ \text{min}^{-1}$ for $t_{DR} = 0$ to 14 min, $k_2 \approx 0.27\ \text{min}^{-1}$ for $t_{DR} = 14$ to 18 min and $k_3 \approx 0.03\ \text{min}^{-1}$ for $t_{DR} = 18$ to 30 min.

3.2.3 XRD profiles of samples

Results of XRD measurements for the $Nd_{12.5}Fe_{73}Co_8B_{6.5}$ and $Nd_{12.5}Fe_{72.8}Co_8B_{6.5}Ga_{0.2}$ alloys at $t_{DR} = 0$, 12, 14, 16 and 18 min are shown in Fig. 8. For both of the $Nd_{12.5}Fe_{73}Co_8B_{6.5}$ and $Nd_{12.5}Fe_{72.8}Co_8B_{6.5}Ga_{0.2}$ alloys, diffraction peaks at $t_{DR} = 0$ min can be assigned NdH_x, Fe_2B and α-Fe phases, which are typical HD reaction products, and diffraction peaks assigned as the $NdFe_4B_4$ phase (B-rich phase) are also observed. However, several peaks observed around $2\theta = 27.7$, 28.7 and 40.4° remain unidentified.

With the progress of the DR reaction, the volume fractions of the NdH_x, Fe_2B and α-Fe phases gradually decreased and that of the $Nd_2Fe_{14}B$ phase increased. Through a careful analysis, it was clear that the NdH_x peaks observed around $2\theta = 28.2°$ remained at $t_{DR} = 14$ min, and these peaks almost disappeared at $t_{DR} = 16$ min for both of the $Nd_{12.5}Fe_{73}Co_8B_{6.5}$ and $Nd_{12.5}Fe_{72.8}Co_8B_{6.5}Ga_{0.2}$ alloys.

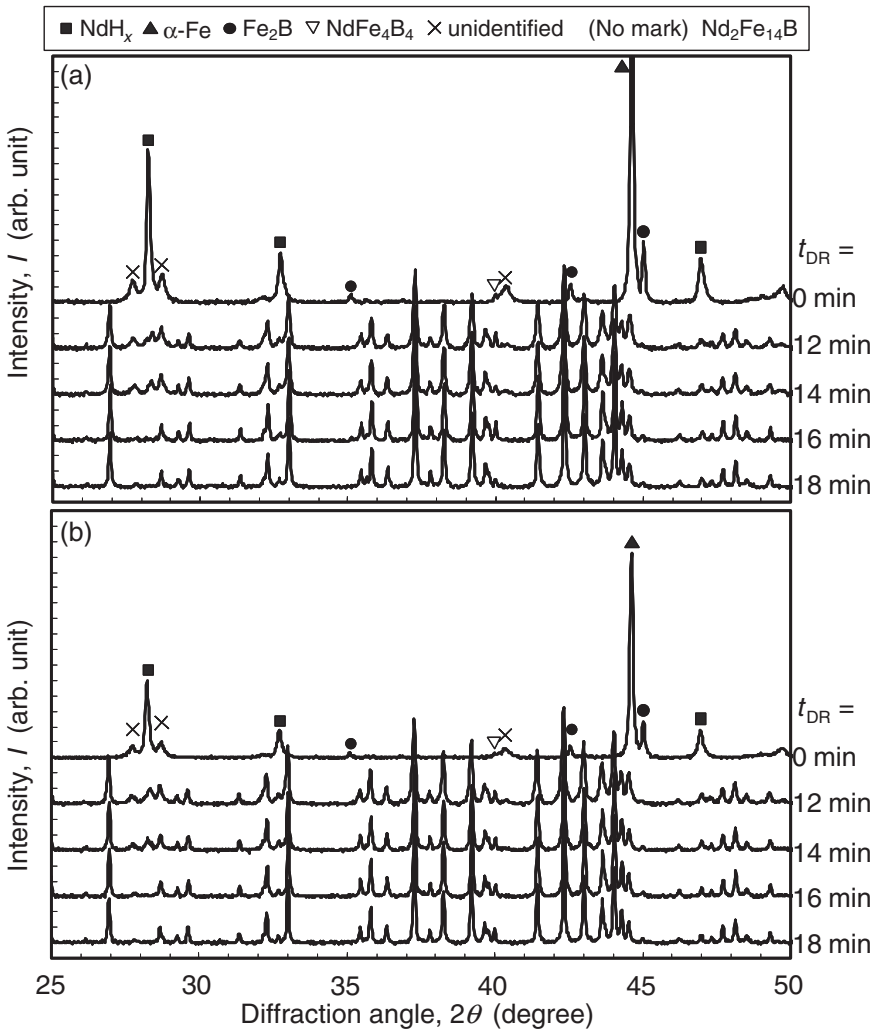

Fig. 8 XRD profiles of samples at various DR treatment time (t_{DR}) for (a) $Nd_{12.5}Fe_{73}Co_8B_{6.5}$ and (b) $Nd_{12.5}Fe_{72.8}Co_8B_{6.5}Ga_{0.2}$ alloys after HD treatment at 840°C for 4 h.

3.2.4 Positron lifetime of samples

Figure 9(a) shows the mean positron lifetime (τ_M) obtained by positron lifetime spectroscopy and Fig. 9(b) shows the variance of fit ($\chi^2 q^{-1}$) of measured spectra for the $Nd_{12.5}Fe_{73}Co_8B_{6.5}$ and $Nd_{12.5}Fe_{72.8}Co_8B_{6.5}Ga_{0.2}$ alloys. From $t_{DR} = 0$ to 12 min, the values of τ_M and $\chi^2 q^{-1}$ for $Nd_{12.5}Fe_{72.8}Co_8B_{6.5}Ga_{0.2}$ were nearly equal to those for $Nd_{12.5}Fe_{73}Co_8B_{6.5}$, whereas considerable differences in both τ_M and $\chi^2 q^{-1}$ between the two alloys arise at $t_{DR} = 14$ min, when significant differences in H_{cJ} were observed between the two alloys, as shown in Figs. 5 and 6.

4. Discussion

4.1 Relationship between microstructure, coercivity and positron lifetime during extended DR treatment (Stage IV)

At room temperature, the typical diffusion length of a positron after thermalization until annihilation in a perfect metal crystal is on the order of 10^{-7} m, which is on the same scale as the typical grain size of HDDR-processed Nd-Fe-B alloys with high coercivity obtained in Stage III. Therefore, most positrons injected into a sample annihilate with electron in the matrix before reaching the grain boundary if the grain size of the sample is much larger than 100 nm. On the contrary, if the grain size of the sample is on the order of 100 nm, most positrons can diffuse to the grain boundary and are trapped. The lifetime of positrons at the grain boundary is generally longer than that in the matrix, due to the locally reduced electron density.

As shown in Fig. 4, in Stage IV, the grain size of the alloy increased to such an extent with DR time that the number of positrons that annihilated in the matrix before arriving at the grain boundary could not be neglected. As a result, it was observed in Stage IV that the measured mean positron lifetime decreased with the DR time, as shown in Fig. 9, because positrons that annihilate in the matrix have a shorter lifetime. These results can be explained by the fact that τ_M at $t_{DR} = 480$ min (155 ps) closely corresponded to the lifetime of alloy before HDDR treatment (157 ps) with a grain size of 100 μm or more.

Mäkinen *et al.*[16] estimated the positron lifetime in a sintered Nd-Fe-B alloy by low-temperature positron lifetime measurements and concluded that the positron lifetime in the $Nd_2Fe_{14}B$ crystal was about 157 ps. In the present study, τ_M at $t_{DR} = 480$ min also closely agreed with the result of Mäkinen *et al.*

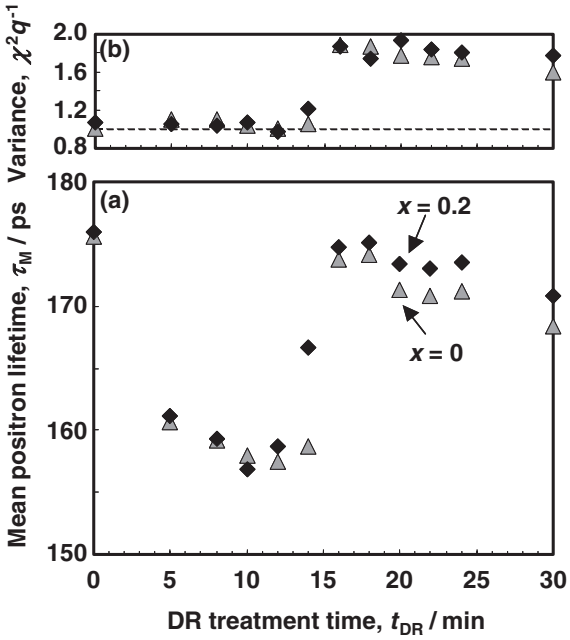

Fig. 9 Results of positron lifetime spectroscopy of samples at various DR treatment time (t_{DR}) for $Nd_{12.5}Fe_{73-x}Co_8B_{6.5}Ga_x$ ($x = 0, 0.2$) alloys after HD treatment at 840°C for 4 h: (a) mean positron lifetime (τ_M), (b) variance ($\chi^2 q^{-1}$).

4.2 Detection of change of grain boundary in period of developing coercivity (Stage II) by positron lifetime spectroscopy

As shown in Figs. 5 and 6, there is a small difference between $Nd_{12.5}Fe_{73}Co_8B_{6.5}$ and $Nd_{12.5}Fe_{72.8}Co_8B_{6.5}Ga_{0.2}$ alloys in the DR period in which the sharp increase in coercivity is observed. $Nd_{12.5}Fe_{73}Co_8B_{6.5}$ alloy at $t_{DR} =$ 14 min retains a low H_{cJ}, but the $Nd_{12.5}Fe_{72.8}Co_8B_{6.5}Ga_{0.2}$ alloy at the same t_{DR} (= 14 min) shows a slightly increased H_{cJ} to 102 kA/m in comparison with that at $t_{DR} = 12$ min (48 kA/m).

In this study, the results of TDS and XRD did not reflect the difference in coercivity of these two alloys at $t_{DR} =$ 14 min. On the other hand, positron lifetime measurements clearly revealed the difference between two alloys at $t_{DR} =$ 14 min. At this moment, $\chi^2 q^{-1}$ of $Nd_{12.5}Fe_{73}Co_8B_{6.5}$ alloy remained around 1.0. However, $\chi^2 q^{-1}$ of the $Nd_{12.5}Fe_{72.8}Co_8B_{6.5}Ga_{0.2}$ alloy increased to 1.2 at the same moment, when H_{cJ} slightly increased. $Nd_{12.5}Fe_{72.8}Co_8B_{6.5}Ga_{0.2}$ alloy also showed higher τ_M than $Nd_{12.5}Fe_{73}Co_8B_{6.5}$ alloy at $t_{DR} = 14$ min. These results strongly suggest that the Nd-rich intergranular phases partially form at $t_{DR} = 14$ min only in the $Nd_{12.5}Fe_{72.8}Co_8B_{6.5}Ga_{0.2}$ alloy. Positrons should be trapped and annihilated around these Nd-rich phases. These results clearly show that positron lifetime spectroscopy is a more sensitive probe for the study of microstructural changes around the Nd-rich intergranular phases in the Nd-Fe-B alloys. Therefore, the positron annihilation method can help to obtain a deeper understanding of the mechanism of coercivity development in the HDDR-processed Nd-Fe-B-based magnets.

Moreover, the mean positron lifetimes in the samples processed by HD treatment for both alloys before DR treatment (*i.e.*, $t_{DR} = 0$ min) were much larger than 157 ps, because most of positrons annihilate at boundaries in the disproportionation mixture. When the samples were subjected to DR treatment, the mean positron lifetimes decreased with DR time to approach to 157 ps. This is attributed to the increase in the volume fraction of the $Nd_2Fe_{14}B$ phase, which is the recombination reaction product. It is noteworthy that the measured mean positron lifetimes at $t_{DR} = 10$ and 12 min for both the alloys were nearly equal to the positron lifetime in the bulk $Nd_2Fe_{14}B$ phase (157 ps) as described above, although the $Nd_2Fe_{14}B$ phase was composed of very fine grains and the specific area of grain boundaries or interfaces between $Nd_2Fe_{14}B$ phase and remnant disproportionated phase such as α-Fe and NdH_x phases was extremely large. This means that the local electron density of the grain boundary was not considerably reduced; in other words, the coherency of the grain boundary (or interface) was high. On the contrary, the observed abrupt increases in mean positron lifetimes for both the alloys in Stage II show that the coherency of the grain boundary was decreased by the precipitation of the Nd-rich intergranular phase ($t_{DR} =$ 12 min).

In our previous studies,[6–8] Nd-rich intergranular phases could be detected only after the NdH_x phases had disappeared. However, in the present study, the formation of a small amount of the Nd-rich intergranular phases during the DR process, which was detected by positron lifetime spectroscopy, contributed to the onset of coercivity in the $Nd_{12.5}Fe_{72.8}Co_8B_{6.5}Ga_{0.2}$ alloy at $t_{DR} = 14$ min, even if the NdH_x phases remained.

5. Conclusions

Positron lifetime spectroscopy was able to detect very sensitively the possible changes in the grain boundary region that caused the onset of coercivity attributed to the formation of Nd-rich intergranular phases, in comparison with TDS and XRD analysis. After the onset of coercivity during DR treatment, the change in positron lifetime closely corresponded to the change in intrinsic coercivity (H_{cJ}) with the progress of DR treatment, which could be explained in terms of the grain sizes of the recombined $Nd_2Fe_{14}B$ phases and the diffusion length of positron annihilation in the matrix without being trapped in the grain boundary region. Furthermore, it was shown that formation of a small amount of the Nd-rich intergranular phases during DR process, which was detected only by positron lifetime spectroscopy, contributed to the onset of coercivity, even when NdH_x phases remained.

Acknowledgements

The authors would like to thank Mr. Y. Yamaguchi for his helpful experimental assistance.

This work was partly supported by the "Global COE (Centers of Excellence) Program" and "Elements Science and Technology Project" for "High performance anisotropic nanocomposite permanent magnets with low rare-earth content", from the Ministry of Education, Culture, Sports, Science and Technology, Japan.

REFERENCES

1) P. Hautojaervi: *Positrons in Solids*, (Springer-Verlag, Berlin, Heidelberg, New York, 1979).
2) W. Brandt and A. Dupasquier: *Positron Solid-State Physics*, (North Holland Publishing Company, Amsterdam, New York, Oxford, 1983).
3) A. Dupasquier and A. P. Mills, Jr.: *Positron Spectroscopy of Solids*, (IOS Amsterdam, Oxford, Tokyo, Washington DC, 1995).
4) T. Takashita and R. Nakayama: Proc. 10th Int. Workshop on Rare Earth Magnets and their Applications, Vol. 1 (1989) pp. 551–557.
5) R. Nakayama and T. Takeshita: J. Alloy. Compd. **193** (1993) 259–261.
6) T. Nishiuchi, S. Hirosawa, M. Nakamura, M. Kakimoto, T. Kawabayashi, H. Araki and Y. Shirai: IEEJ Trans. Electr. Electr. Eng. **3** (2008) 390–393.
7) T. Nishiuchi, S. Sakashita, S. Hirosawa, M. Nakamura, M. Kakimoto, T. Kawabayashi, M. Mizuno, H. Araki and Y. Shirai: Proc. 20th Int. Workshop on Rare Earth Magnets and their Applications, (2008) pp. 77–79.
8) T. Nishiuchi, S. Sakashita, S. Hirosawa, M. Nakamura, M. Kakimoto, T. Kawabayashi, M. Mizuno, H. Araki and Y. Shirai: J. Magn. Magn. Mater., published online (DOI:10.1016/j.jmmm.2009.09.031).
9) P. Kirkegaard and M. Eldrup: Comput. Phys. Commun. **3** (1972) 240–255.
10) P. Kirkegaard and M. Eldrup: Comput. Phys. Commun. **7** (1974) 401–409.
11) P. Kirkegaard, M. Eldrup, O. E. Mogensen and N. J. Pedersen: Comput. Phys. Commun. **23** (1981) 307–335.
12) W. F. Li, T. Ohkubo, K. Hono, T. Nishiuchi and S. Hirosawa: Appl. Phys. Lett. **93** (2008) 052505.
13) W. F. Li, T. Ohkubo, K. Hono, T. Nishiuchi and S. Hirosawa: J. Appl. Phys. **105** (2009) 07A706.
14) M. Uehara, T. Tomida, H. Tomizawa, S. Hirosawa and Y. Maehara: J. Magn. Magn. Mater. **159** (1996) L304–L308.
15) H. Nakamura, K. Kato, D. Book, S. Sugimoto, M. Okada and M. Homma: IEEE Trans. Magn. **35** (1999) 3274–3276.
16) S. Mäkinen, O.-P. Kähkönen and M. Manninen: J. Phys. Cond. Matter. **3** (1991) 2507–2514.